arXiv:1604.08527v1 [cond-mat.str-el] 28 Apr 2016

Indication of the fermion condensation in a strongly correlated electron system in SiGe/Si/SiGe quantum wells

M. Yu. Melnikov,[1] A. A. Shashkin,[1] V. T. Dolgopolov,[1] S.-H. Huang,[2] C. W. Liu,[2] and S. V. Kravchenko[3]

[1]*Institute of Solid State Physics, Chernogolovka, Moscow District 142432, Russia*
[2]*Department of Electrical Engineering and Graduate Institute of Electronics Engineering, National Taiwan University, Taipei 106, Taiwan, and National Nano Device Laboratories, Hsinchu 300, Taiwan*
[3]*Physics Department, Northeastern University, Boston, Massachusetts 02115, USA*

Using two-dimensional electron system in ultra-high quality SiGe/Si/SiGe quantum wells, we experimentally compare the product of the Lande g-factor and the *energy-averaged* effective mass, $g_F m$, with that at the Fermi level, $g_F m_F$, and verify that the behaviors of these measured values are qualitatively different. With decreasing electron density (or increasing interaction strength), the product $g_F m_F$ monotonically increases in the entire range of electron densities, while the product $g_F m$ saturates at low densities, in agreement with theoretical predictions. This reveals a precursor to the long-sought-for fermion condensation in this electron system. The results indicate the occurrence of a new state of matter.

PACS numbers: 71.10.Hf, 71.27.+a, 71.10.Ay

The behavior of strongly-correlated fermions in two dimensions is a forefront area of modern condensed matter physics in which theoretical methods are still poorly developed and new experimental results are of great interest. According to theoretical calculations [1–5], as the strength of fermion-fermion interaction is increased, the single-particle spectrum becomes progressively flatter in the vicinity of the Fermi energy (see inset to Fig. 1) eventually forming a plateau: the fermions "condense". The flattening of the spectrum is related to the increase of the effective fermion mass m_F at the Fermi level. The condensation of fermions, previously never observed experimentally, is similar to the condensation of bosons responsible for such prominent phenomena as superconductivity and superfluidity; the important difference, however, is that, unlike the condensation of bosons, the fermion condensation occurs at the Fermi level in a range of momenta.

The role of electron-electron interactions in the behavior of two-dimensional (2D) electron systems increases as the electron density is decreased. The interaction strength is characterized by the Wigner-Seitz radius, $r_s = 1/(\pi n_s)^{1/2} a_B$ (here n_s is the electron density and a_B is the effective Bohr radius in semiconductor), which in the single-valley case is equal to the ratio of the Coulomb and kinetic energies. At high electron densities, where $r_s \sim 1$, interactions are not prevalent; 2D electron systems exhibit metallic conductivity and their behavior can be well described by the Fermi liquid theory. In the opposite limit of low electron densities ($r_s > 35$) interactions are dominant, and the electrons are expected to form a Wigner crystal [6, 7]. At intermediate values of r_s, where the energy of interactions exceeds all other energy scales but is still not high enough to cause the electrons to crystallize, different scenarios of the system behavior were suggested theoretically, and numerous experiments on different electron systems were performed (see reviews [8–10]). Nevertheless, the behavior of the strongly interacting 2D electron system is still not well understood. One of the important points is the residual scattering potential. Even in quite perfect electron systems the electron properties are influenced by the residual disorder [11–13]. At present, it is unclear whether the clean limit (*i.e.*, the limit in which the influence of disorder on the electron properties is negligible) has been reached in experiments on the least disordered electron systems. Finally, there exist experimental facts that contradict both intuitive expectations and calculations, *e.g.*, a decrease of the effective mass in fully spin-polarized single-valley electron systems [14, 15]. All this means that new experimental data are needed on the behavior of strongly interacting 2D electron systems as close as possible to the ideal ones in the sense of both strength of electron-electron interactions and weakness of the scattering potential.

Raw experimental data obtained in strongly correlated 2D electron systems can be divided into two groups: (i) data describing the electron system as a whole, like the magnetic field required to fully polarize electron spins, thermodynamic density of states, or magnetization of the electron system, and (ii) data related solely to the electrons at the Fermi level, like the amplitude of the Shubnikov-de Haas oscillations yielding the effective mass m_F and Lande g-factor g_F at the Fermi level. As a rule, the data in the first group are interpreted using the quasiparticle language in which the energy-averaged values of effective mass, m, and Lande g-factor, g, are used. To determine the values, the formulas that hold for the case of non-interacting electrons are employed. Although this approach is ideologically incorrect, the results for m and g often turn out to be the same as the results for m_F and g_F. Particularly, simultaneous increase of the energy-averaged effective mass and that at the Fermi level was reported in earlier publications [8–10, 16, 17].

In this paper, we experimentally compare the product of the Lande g-factor and the *energy-averaged* effective mass, $g_F m$, with that at the Fermi level, $g_F m_F$. It turns out that the behaviors of these measured values are qualitatively different: with decreasing electron density, n_s, the product $g_F m_F$ monotonically increases in the entire range of electron densities, while the product $g_F m$ saturates at low n_s. This reveals a precur-

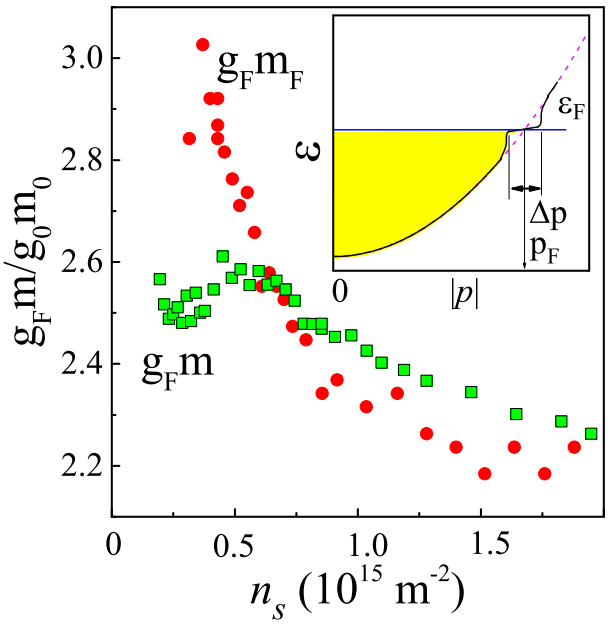

FIG. 1: Product of the Lande factor and effective mass as a function of electron density determined by measurements of the field of full spin polarization (squares) and Shubnikov-de Haas oscillations (dots) at $T \approx 30$ mK. ($g_0 = 2$ and $m_0 = 0.19m_e$ are the values for noninteracting electrons). The inset shows schematically the single-particle spectrum of the electron system in a state preceding the fermion condensation (solid black line). The dashed violet line corresponds to an ordinary parabolic spectrum. The occupied electron states at $T = 0$ are indicated by the shaded area.

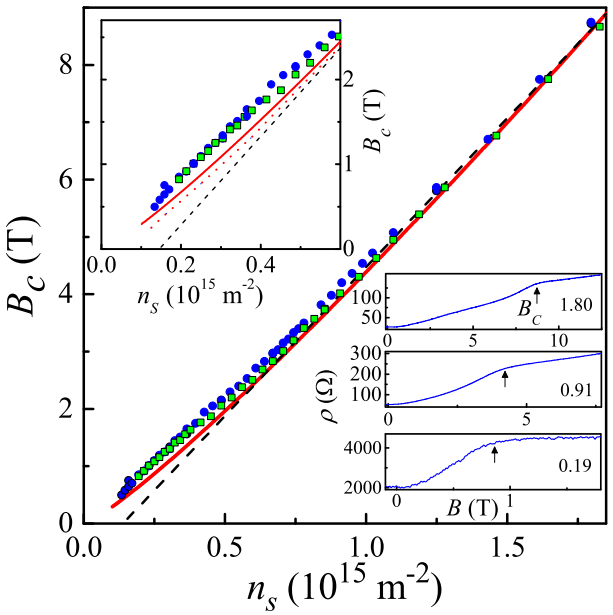

FIG. 2: Dependence of the field of complete spin polarization on electron density at a temperature of 30 mK for two samples (dots and squares). The dashed black line is a linear fit to the high-density data which extrapolates to zero at a density n_c. The solid red line corresponds to the calculation [23] for the clean limit. Top inset: the low density region of the main figure on an expanded scale. Also shown by the dotted red line is the calculation [23] taking into account the electron scattering. Bottom inset: the parallel-field magnetoresistance at a temperature of 30 mK at different electron densities indicated in units of 10^{15} m^{-2}. The polarization field B_c is marked by arrows.

sor to the fermion condensation in this electron system and indicates the occurrence of a new state of matter.

Samples were prepared based on a 15 nm SiGe/Si/SiGe quantum well grown in an ultrahigh-vacuum chemical-vapor-deposition (UHVCVD) [18, 19]. The Hall-bar samples with width 50 μm and the distance between potential probes 150 μm were patterned using standard photo-lithography. Contacts consisted of AuSb alloy, deposited in a thermal evaporator in vacuum and annealed for 5 minutes in N_2 atmosphere at 440°C. Next, approximately 300 nm thick layer of SiO was deposited in a thermal evaporator and a $>$ 20 nm thick Al gate was deposited on top of SiO. No mesa etching was used, and the 2D electron gas was created in a way similar to silicon metal-oxide-semiconductor field-effect transistors (MOSFETs) (for details, see Ref. [20, 21]). The maximum electron mobility in our samples reached 240 m^2/Vs which is the highest mobility ever reported in this electron system [21].

Measurements were made in an Oxford TLM-400 dilution refrigerator in a temperature range 0.03 – 1.2 K. The resistance was measured by a standard four-terminal lock-in technique in a frequency range 1 – 11 Hz. The applied currents varied in the range 0.5 – 4 nA. We used a saturating infrared illumination to improve the quality of the contacts and increase the electron mobility. This did not affect the electron density at a fixed gate voltage.

We have studied the magnetic field of the complete polarization of the electron spins, yielding the energy-averaged product $g_F m$, and Shubnikov-de Haas oscillations, yielding the product $g_F m_F$ at the Fermi level (Fig. 1). The parallel-field magnetoresistance (ı.e., magnetoresistance measured in the configuration where the magnetic field is parallel to the 2D plane) has been studied in the perpendicular orientation of the magnetic field and the current. In this case, the shape of the experimental dependences is the closest to that expected theoretically [22]. The field of the full spin polarization, B_c, corresponds to a distinct "knee" of the experimental dependences followed by the saturation of the resistance (see the bottom inset to Fig. 2).

The magnetic field of the complete spin polarization as a function of electron density is shown in Fig. 2 for two samples. Over the electron density range 0.7×10^{15} m$^{-2} < n_s < 2 \times 10^{15}$ m^{-2}, the data are described well by a linear dependence that extrapolates to zero at $n_c \approx 0.14 \times 10^{15}$ m^{-2} (dashed black line). At lower electron densities, however, the experimental dependence $B_c(n_s)$ deviates from the straight line, and its linear extrapolation hits the origin. The solid red line in Fig. 2 shows the polarization field $B_c(n_s)$ calculated using the quantum Monte Carlo method [23]. The experimental results are in good agreement with the theoretical calculations for the clean limit $k_F l \gg 1$ (here k_F is the

Fermi wavelength and l is the mean free path), assuming that the Lande g-factor, renormalized by electron-electron interactions, is equal to 2.4. Although in Ref. [23] Lande g-factor was equal to 2, the reason for the 20% discrepancy between the theory and experiment may be due to the finite size of the electron wave function in the direction perpendicular to the interface. Besides, the product $k_F l$ decreases with decreasing electron density, which leads to a downward deviation in the theoretical dependence, as shown by the dotted red line in the upper inset to Fig. 2.

To check whether or not the residual disorder affects the results for the magnetic field of complete spin polarization, we compare our data with those previously obtained on samples with an order of magnitude lower mobility [24]. At high electron densities, the dependence $B_c(n_s)$ in Ref. [24] is also linear and extrapolates to zero at a finite density; the slope of the dependence is equal to 6×10^{-15} T·m^2 and is close to the slope 5.4×10^{-15} T·m^2 observed in our experiment. However, the offset $n_c \approx 0.3 \times 10^{15}$ m^{-2} of Ref. [24] is appreciably higher compared to our case. Therefore, the behavior of the polarization field B_c is affected by the disorder potential in accordance with Ref. [23]. Good agreement between our experimental data for B_c and the calculations for the clean limit [23] gives evidence that the electron properties studied in our samples are only weakly sensitive to the residual disorder and the clean limit has been reached in our samples.

The product $g_F m$ that characterizes the whole 2D electron system can be determined from the equality of the Zeeman splitting and the Fermi energy of the spin-polarized electron system

$$g_F \mu_B B_c = \frac{2\pi\hbar^2 n_s}{m g_v}, \qquad (1)$$

where $g_v = 2$ is the valley degeneracy and μ_B is the Bohr magneton.

On the other hand, the Lande g-factor g_F and effective mass m_F *at the Fermi level* can be determined by the analysis of the Shubnikov-de Haas oscillations in relatively weak magnetic fields

$$\begin{aligned} A &= \sum_i A_i^{LK} \cos\left[\pi i \left(\frac{\hbar c \pi n_s}{eB_\perp} - 1\right)\right] Z_i^s Z_i^v \\ A_i^{LK} &= 4 \exp\left(-\frac{2\pi^2 i k_B T_D}{\hbar\omega_c}\right) \frac{2\pi^2 i k_B T/\hbar\omega_c}{\sinh\left(2\pi^2 i k_B T/\hbar\omega_c\right)} \\ Z_i^s &= \cos\left(\pi i \frac{\Delta_Z}{\hbar\omega_c}\right) = \cos\left(\pi i \frac{g_F m_F}{2m_e}\right) \\ Z_i^v &= \cos\left(\pi i \frac{\Delta_v}{\hbar\omega_c}\right), \end{aligned} \qquad (2)$$

where T_D is the Dingle temperature, T is the temperature, m_e is the free electron mass, $\hbar\omega_c$ is the cyclotron splitting, Δ_Z is the Zeeman splitting, and Δ_v is the valley splitting. It is clear from the relation (2) that as long as one sets $Z_i^v = 1$ in the range of magnetic fields studied, the fitting parameters are $T_D m_F$, m_F, and $g_F m_F$. The values $T_D m_F$ and m_F are obtained in the temperature range where the spin splitting is insignificant; the detailed results for the effective mass will be published elsewhere. Being weakly sensitive to these two fitting parameters, the shape of the fits at the lowest temperatures turns out to be very sensitive to the product $g_F m_F$. The quality of the fits is demonstrated in Fig. 3. The magnetoresistance $\delta\rho_{xx} = \rho_{xx} - \rho_0$ normalized by ρ_0 (where ρ_0 is the monotonic change of the dissipative resistivity with magnetic field) is described well using Eq. (2).

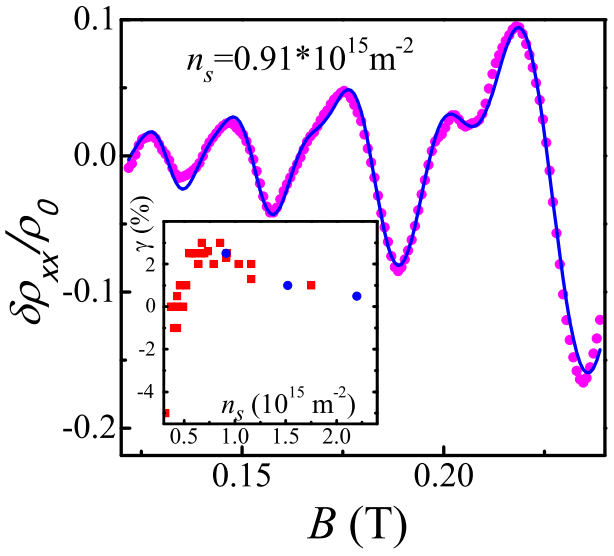

FIG. 3: Fit of the normalized magnetoresistance $\delta\rho_{xx}/\rho_0$ at a temperature of ≈ 30 mK (dots) using Eq. (2) with $g_F^* m_F^*/m_e = 0.905$, $T_D = 0.12$ K, $m_F^* = 0.25 m_e$, and $\gamma = 2.5\%$. Inset: the asymmetry coefficient γ versus electron density for two samples. The Dingle temperature for two spin subbands is found to be different in our samples, similar to the results of Ref. [25]. Although the effect is appreciably weaker in our case, we have to introduce another fitting parameter γ for $T_D^{u,d} = T_D(1 \pm \gamma)$. The difference between the Dingle temperatures for two spin subbands does not exceed 6%, the Dingle temperature for energetically favorable spin direction being smaller over the range of electron densities 0.6×10^{15} m^{-2} $< n_s < 2 \times 10^{15}$ m^{-2}, whereas at lower densities the quantity γ changing sign.

The main result of our study is shown in Fig. 1: the products of the average $g_F m$ and $g_F m_F$ at the Fermi level behave similarly at high electron densities, where electron-electron interactions are relatively weak, but differ at low densities, where the interactions become especially strong. The product $g_F m_F$ monotonically increases as the electron density is decreased in the entire range of electron densities, while the product $g_F m$ saturates at low n_s. We emphasize that it is the qualitative difference in the behaviors of the two sets of data that matters, rather than comparison of the absolute values.

The experimental results are naturally interpreted as follows. According to the concept of fermion condensation [5], with increasing strength of electron-electron interactions, the single-particle spectrum flattens in a region Δp near the Fermi momentum p_F (inset to Fig. 1). At relatively high electron

densities $n_s > 0.7 \times 10^{15}$ m^{-2}, this effect is not important since the single-particle spectrum does not change noticeably in the interval Δp and the behaviors of the energy-averaged effective mass and that at the Fermi level are practically the same. Decreasing the electron density in the range 0.3×10^{15} m$^{-2} < n_s < 0.7 \times 10^{15}$ m^{-2} gives rise to the flattening of the spectrum so that the effective mass at the Fermi level, $m_F = p_F/V_F$, continues to increase (here V_F is the Fermi velocity). In contrast, the energy-averaged effective mass does not, being not particularly sensitive to this flattening. The increase of m_F is restricted by the limiting value determined by temperature: $m_F < p_F \Delta p/4k_B T$. In our experiments, the increase of m_F reaches a factor of about two at $n_s = 0.3 \times 10^{15}$ m^{-2} and $T \approx 30$ mK, which allows one to estimate the ratio $\Delta p/p_F \sim 0.06$. It is the smallness of the interval Δp that provides good agreement between the calculation [23] and our experiment. Near the density n_c, the electron system is in a critical region in which the effective mass at the Fermi level is temperature dependent. A weak decrease of the value $g_F m_F$ with temperature is indeed observed at the lowest-density point in Fig. 1. Altogether, our experimental results show that we have observed a precursor to the fermion condensation in our samples.

This work was supported by RFBR 15-02-03537 and 16-02-00404, RAS, and the Russian Ministry of Sciences. NTU Group was supported by Ministry of Science and Technology (104-2622-8-002-003). S.V.K. was supported by NSF Grant No. 1309337 and BSF Grant No. 2012210.

[1] Khodel, V. A. & Shaginyan, V. R. Superfluidity in system with fermion condensate. *JETP Lett.* **51**, 553-555 (1990).

[2] Volovik, G. E. A new class of normal Fermi liquids. *JETP Lett.* **53**, 222-225 (1991).

[3] Nozières, P. Properties of Fermi liquids with a finite range interaction. *J. Phys. I (France)* **2**, 443-458 (1992).

[4] Zverev, M. V., Khodel, V. A. & Pankratov, S. S. Microscopic theory of a strongly correlated two-dimensional electron gas. *JETP Lett.* **96**, 192-202 (2012).

[5] Amusia, M. Ya., Popov, K. G., Shaginyan, V. R. & Stephanovich, V. A. *Theory of Heavy Fermion Compounds* (Springer, Berlin, 2014).

[6] Chaplik, A. V. Possible crystallization of charge carriers in low-density inversion layers. *Sov. Phys. JETP* **35**, 395-398 (1972).

[7] Tanatar, B. & Ceperley, D. M. Ground state of the two-dimensional electron gas. *Phys. Rev. B* **39**, 5005-5016 (1989).

[8] Kravchenko, S. V. & Sarachik, M. P. Metal-insulator transition in two-dimensional electron systems. *Rep. Prog. Phys.* **67**, 1-44 (2004).

[9] Shashkin, A. A. Metal-insulator transitions and the effects of electron-electron interactions in two-dimensional electron systems. *Phys. Usp.* **48**, 129-149 (2005).

[10] Pudalov, V. M. Metal-insulator transitions and related phenomena in a strongly correlated two-dimensional electron system. *Phys. Usp.* **49**, 203-208 (2006).

[11] Vitkalov, S. A., Sarachik, M. P. & Klapwijk, T. M. Spin polarization of strongly interacting two-dimensional electrons: The role of disorder. *Phys. Rev. B* **65**, 201106(R) (2002).

[12] Vakili, K., Shkolnikov, Y. P., Tutuc, E., De Poortere, E. P. & Shayegan, M. Spin susceptibility of two-dimensional electrons in narrow AlAs quantum wells. *Phys. Rev. Lett.* **92**, 226401 (2004).

[13] Pudalov, V. M., Brunthaler, G., Prinz, A., & Bauer, G. Weak anisotropy and disorder dependence of the in-plane magnetoresistance in high-mobility (100) Si-inversion layers. *Phys. Rev. Lett.* **88**, 076401 (2002).

[14] Padmanabhan, M., Gokmen, T., Bishop, N. C. & Shayegan, M. Effective mass suppression in dilute, spin-polarized two-dimensional electron systems. *Phys. Rev. Lett.* **101**, 026402 (2008).

[15] Gokmen, T., Padmanabhan, M., Vakili, K., Tutuc, E. & Shayegan, M. Effective mass suppression upon complete spin-polarization in an isotropic two-dimensional electron system. *Phys. Rev. B* **79**, 195311 (2009).

[16] Dolgopolov, V. T. Two-dimensional electrons in (100)-oriented silicon field-effect structures in the region of low concentrations and high mobilities. *JETP Lett.* **101**, 282-287 (2015).

[17] Mokashi, A., Li, S., Wen, B., Kravchenko, S. V., Shashkin, A. A., Dolgopolov, V. T., & Sarachik, M. P. Critical behavior of a strongly interacting 2D electron system. *Phys. Rev. Lett.* **109**, 096405 (2012).

[18] Lu, T. M., Tsui, D. C., Lee, C.-H. & Liu, C. W. Observation of two-dimensional electron gas in a Si quantum well with mobility of 1.6x106 cm2/Vs. *Appl. Phys. Lett.* **94**, 182102 (2009).

[19] Lu, T. M., Tsui, D. C., Lee, C.-H. & Liu, C. W. Erratum: Observation of two-dimensional electron gas in a Si quantum well with mobility of 1.6x106 cm2/Vs [Appl. Phys. Lett.94, 182102 (2009)]. *Appl. Phys. Lett.* **97**, 059904 (2010).

[20] Melnikov, M. Yu., Shashkin, A. A., Dolgopolov, V. T., Kravchenko, S. V., Huan, S.-H. & Liu, C. W. Effective electron mass in high-mobility SiGe/Si/SiGe quantum wells. *JETP Lett.* **100**, 114-119 (2014).

[21] Melnikov, M. Yu., Shashkin, A. A., Dolgopolov, V. T., Huan, S.-H., Liu, C. W. & Kravchenko, S. V. Ultra-high mobility two-dimensional electron gas in a SiGe/Si/SiGe quantum well. *Appl. Phys. Lett.* **106**, 092102 (2015).

[22] Dolgopolov, V. T. & Gold, A. Magnetoresistance of a two-dimensional electron gas in a parallel magnetic field. *JETP Lett.* **71**, 27-30 (2000).

[23] Fleury, G. & Waintal, X. Energy scale behind the metallic behaviors in low-density Si MOSFETs. *Phys. Rev. B* **81**, 165117 (2010).

[24] Lu, T. M., Sun, L., Tsui, D. C., Lyon, S., Pan, W., Muehlberger, M., Shaeffler, F., Liu, J. & Xie, Y. H. In-plane field magnetoresistivity of Si two-dimensional electron gas in Si/SiGe quantum wells at 20 mK. *Phys. Rev. B* **78**, 233309 (2008).

[25] Pudalov, V. M., Gershenson, M. E. & Kojima, H. Probing electron interactions in a two-dimensional system by quantum magneto-oscillations. *Phys. Rev. B* **90**, 075147 (2014).